ACS chemical biology

Articles

pubs.acs.org/acschemicalbiology

Small Molecule Probe Suitable for *In Situ* Profiling and Inhibition of Protein Disulfide Isomerase

Jingyan Ge,[†] Chong-Jing Zhang,[†] Lin Li,[†] Li Min Chong,[†] Xiaoyuan Wu,[†] Piliang Hao,[‡] Siu Kwan Sze,[‡] and Shao Q. Yao*[,†]

[†]Department of Chemistry, National University of Singapore, 3 Science Drive 3, Singapore 117543

[‡]School of Biological Sciences, Nanyang Technological University, 60 Nanyang Drive, Singapore 637551

Supporting Information

ABSTRACT: Proper folding of cellular proteins is assisted by protein disulfide isomerases (PDIs) in the endoplasmic reticulum of mammalian cells. Of the at least 21 PDI family members known in humans, the 57-kDa PDI has been found to be a potential therapeutic target for a variety of human diseases including cancer and neurodegenerative diseases. Consequently, small molecule PDI-targeting inhibitors have been actively pursued in recent years, and thus far, compounds possessing moderate inhibitory activities (IC_{50} between 0.1 and 100 μM against recombinant PDI) have been discovered. In this article, by using *in situ* proteome profiling experiments in combination with *in vitro* PDI enzymatic inhibition assays, we have discovered a phenyl vinyl sulfonate-containing small molecule (**P1**; shown) as a relatively potent and specific inhibitor of endogenous human PDI in several mammalian cancer cells (e.g., $GI_{50} \sim 4$ μM). It also possesses an IC_{50} value of 1.7 ± 0.4 μM in an *in vitro* insulin aggregation assay. Our results indicate **P1** is indeed a novel, cell-permeable small molecule PDI inhibitor, and the electrophilic vinyl sulfonate scaffold might serve as a starting point for future development of next-generation PDI inhibitors and probes.

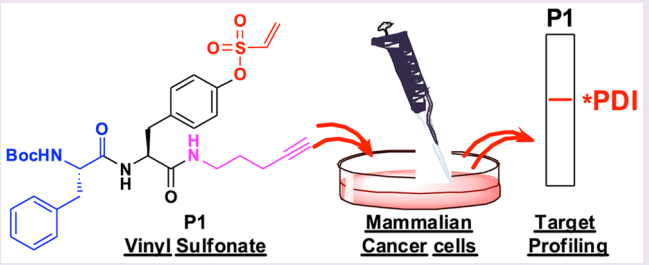

Proper folding of cellular proteins is a highly complex process, and the disulfide bond formation is one of the key steps, which normally takes place in the endoplasmic reticulum (ER) with the assistance of a class of enzymes called protein disulfide isomerases (PDIs).[1] PDIs catalyze the formation (oxidation), breakage (reduction), and rearrangement (isomerization) of disulfide bonds between cysteine residues within proteins as they fold. This allows proteins to quickly find the correct arrangement of disulfide bonds in their fully folded state. Currently, there are at least 21 PDI family members known in humans.[2] One of the best-known human PDIs is PDIA1 (sometimes simply referred to as PDI), a 57-kDa protein residing mostly in the ER, although it can also be released to function at the cell surface or extracellular matrix. Similar to most other family members of PDIs, PDI contains four thioredoxin-like domains (a, b, b′ and a′), two of which possess a canonical CGHC motif, giving rise to the two PDI active sites within the a and a′ catalytic domains (Figure 1A). The other two noncatalytic domains (b and b′) are essential for the noncovalent binding of incompletely folded protein substrates.[3] The four cysteine residues in PDI ($Cys^{53/56}$ and $Cys^{397/400}$) have been shown to possess unusually high/low pK_a values, which is critical in maintaining the catalytic activities of PDI and the cycling between the oxidized and reduced states (Figure 1B).[4] In recent years, PDI has been found to play key roles in a wide range of physiological and disease processes.[2] As the key enzyme involved in protein folding, PDI was recently linked to apoptosis of cells in several neurological disorders including Huntington's disease, Alzheimer's disease, and Parkinson's disease.[5] PDI is involved in the cellular immune response by facilitating the loading of antigenic peptides onto MHC class I molecules.[6,7] PDI has also been found to take part in the breaking of bonds on the HIV gp120 protein, which is required for HIV infection of lymphocytes and monocytes.[8] Several studies have shown ER stress and unfolded protein responses can activate PDI expression.[9] Consequently, elevated PDI expression levels have been observed in a variety of human cancers.[2,10]

As a potentially promising druggable target, PDI in recent years has received some attention in drug discovery.[5,11−17] Bacitracin, a dodecapeptide antibiotic, was first reported as an PDI inhibitor in 1981[11] and has been found to inhibit PDI activities in a variety of cellular processes.[10,12,13] With an active concentration in the high micromolar range, this compound is a fairly weak and ineffective PDI inhibitor.[13] Its clinical use was further hampered by its nephrotoxicity, low specificity, and low cell permeability.[14] Its relatively large size also makes it difficult to be further modified synthetically. Juniferdin (Figure 1C), an PDI inhibitor discovered through an high-throughput screening (HTS) effort using collections of natural product libraries, was

Received: April 16, 2013
Accepted: September 16, 2013

   dx.doi.org/10.1021/cb4002602 | *ACS Chem. Biol.* XXXX, XXX, XXX−XXX

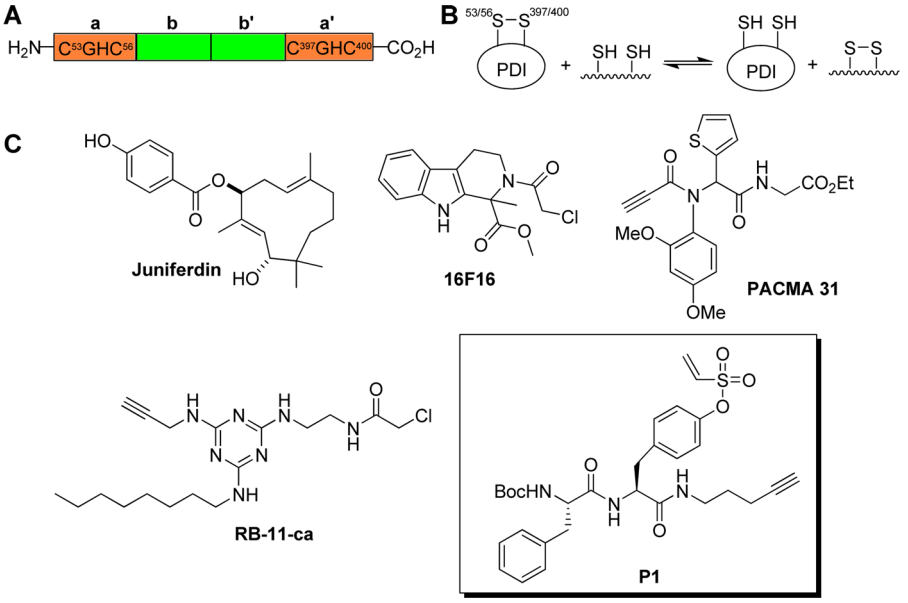

Figure 1. (A) Domain overview of human protein disulfide isomerase (PDI), with the catalytic a and a′ domains (in orange) and the catalytically inactive b and b′ domains (in green). (B) Schematic showing of the PDI-catalyzed reaction. (C) Some known small molecule inhibitors of PDI, as well as **P1** (boxed), the newly discovered PDI inhibitor from the current study.

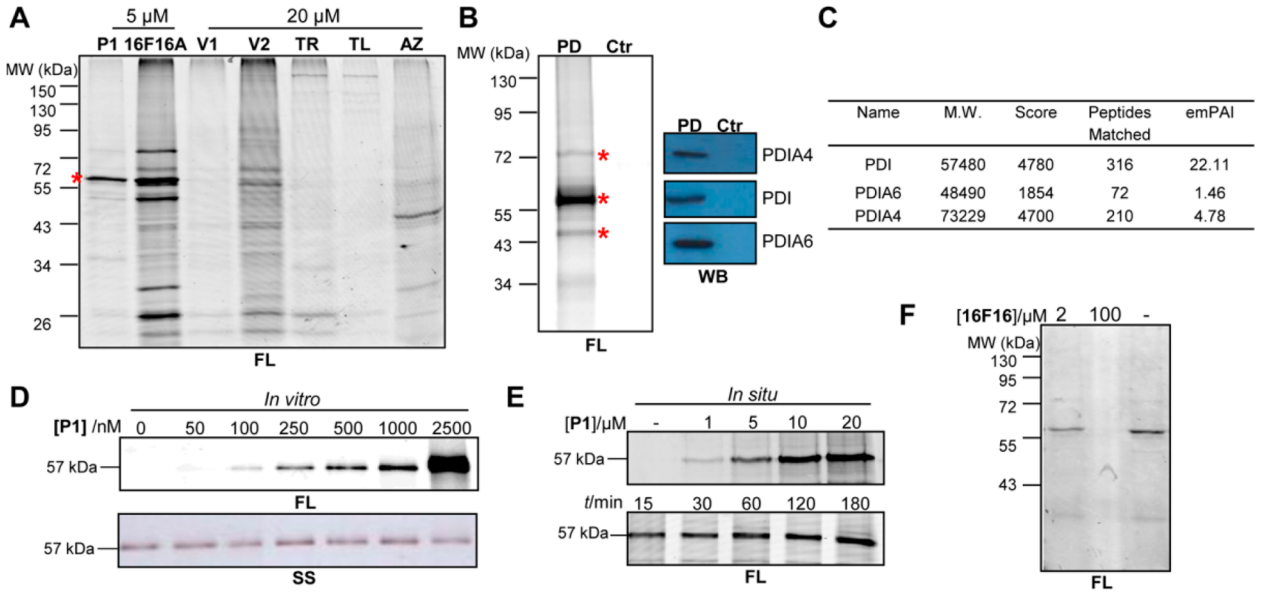

Figure 2. (A) *In situ* proteome reactivity profiles of various electrophilic probes in live MCF-7 cells. For detailed structures of the probes, see SI Figure S1. Upon labeling by each probe (**P1**/16F16A, 5 μM; **V1**/**V2**/**TR**/**TL**/**AZ**, 20 μM), MCF-7 cells were lysed and clicked with Rh−N_3, separated by SDS-PAGE gels followed by in-gel fluorescence scanning (FL). The 57-kDa fluorescent band corresponding to human PDI was labeled (*). (B) *In situ* labeling of MCF-7 cells by **P1**, followed by click chemistry with Rh-Biotin-N_3, pulled-down (PD) by avidin agarose beads, then gel-separated before FL and Western blotting (WB). Control pull-down (PD) was done with DMSO in place of **P1**. (*) The three enriched fluorescent bands were identified as different human PDIs (PDI, PDIA4 and PDIA6) using the corresponding antibodies. (C) LC-MS/MS analysis of the three fluorescent bands (labeled with *) to confirm their identities. (D) Concentration-dependent *in vitro* labeling of purified bovine PDI (25 ng) by **P1**. SS = silver-stained gel. (E) In-gel fluorescence scanning showing both concentration- and time-dependent *in situ* labeling of MCF-7 cells by **P1**. (F) Competitive *in situ* labeling of MCF-7 cells by **P1** (5 μM), with and without pretreatment of 16F16.

found to block the PDI-catalyzed reduction of disulfide bonds in the HIV-1 envelope glycoprotein gp120, thereby inhibiting the entry of HIV-1 virus into cells.[15] The compound showed an IC_{50} value of 156 nM in an *in vitro* insulin aggregation assay. 16F16, another recently discovered PDI inhibitor, was found to suppress apoptosis caused by misfolded proteins in a cell model of Huntington's disease.[5] It possesses an electrophilic chloroacetamide structure that reacted covalently with one (or more) of the four highly nucleophilic cysteine residues within the PDI active sites. In an *in vitro* fluorescence self-quenching assay that uses diabz-GSSG and purified PDI from bovine liver, it exhibited a reported IC_{50} value of ∼70 μM.[5,18] In another study, a compound named PACMA 31, which contains an electrophilic propynoic amide in its core structure, was found to significantly inhibit the growth of ovarian cancer cells through the irreversible inhibition of PDI activity. Subsequent

dx.doi.org/10.1021/cb4002602 | ACS Chem. Biol. XXXX, XXX, XXX−XXX

testing of the compound *in vitro* using recombinant PDI in an insulin aggregation enzymatic assay revealed an IC_{50} value of ~10 μM.[16] Importantly, this compound also exhibited *in vivo* antitumor activities without causing detectable toxicity to normal tissues. While our manuscript was in preparation, Weerapana and co-workers reported the discovery of RB-11-ca, a trifunctionalized 1,3,5-triazine capable of covalently labeling endogenous human PDI (presumably at the Cys^{53} residue) in live HeLa cells.[17] This compound also contains a chloroacetamide moiety and was found to possess similar *in vitro* inhibitory activity as 16F16 against bovine PDI using the fluorescence self-quenching assay, as mentioned above (e.g., IC_{50} values of between 30 and 50 μM).[17] Moreover, RB-11-ca. showed a GI_{50} value of 23.9 μM against HeLa cells in an MTT antiproliferation assay.

We noticed the common structural features of 16F16, PACMA 31 and RB-11-ca, all of which contain electrophilic moieties (e.g., propynoic amide and chloroacetamide), and were therefore highly susceptible to covalent attack by the highly nucleophilic cysteine residues present in the PDI active sites under physiological conditions.[5,16,17] We wondered if other pharmacophores possessing similar kinds of electrophilic groups (e.g., vinyl sulfones,[19,20] β-lactones,[21,22] azanitriles,[23,24] etc.), all of which are known irreversible inhibitors of cysteine-reactive enzymes including cysteine proteases, lipases, and protein tyrosine phosphatases (PTPs), could provide a convenient chemical toolbox for identification of novel PDI inhibitors. We noted that some other recently discovered, biologically interesting compounds might serve the same purpose,[25−27] but they were not included in the current study due to their inaccessibility (to us). Herein, we report the serendipitous discovery of **P1** (boxed compound in Figure 1C), a phenyl vinyl sulfonate-containing small molecule, as a relatively potent and specific inhibitor of endogenous human PDI, capable of killing numerous mammalian cancer cells (GI_{50} ~4 μM). *In vitro* inhibition assay indicated that this compound has an IC_{50} value of 1.7 μM against bovine PDI using insulin aggregation assay and is 40-fold more potent than 16F16 under identical assay conditions. These findings would place **P1** among some of the more potent, cell-permeable small molecule PDI inhibitors discovered to date.

RESULTS AND DISCUSSION

Screening. In order to identify compounds that directly target human PDI *in situ*, we carried out screening in live MCF-7 cells (a human breast cancer cell line) by using the well-established activity-based protein profiling (ABPP) approach.[28−31] This necessitates all compounds to contain a small, chemically benign tag (e.g., a terminal alkyne) that minimizes perturbation to bind PDI *in situ* and at the same time provides a tractable tag for subsequent bioconjugation to reporter-containing azides using click chemistry.[32−35] Of the numerous compounds screened, several representatives were found to possess interesting *in situ* proteome reactivity profiles (Figure 2A; see Figure 1C and Supporting Information (SI) Figure S1); different vinyl sulfone/sulfonate-containing compounds (**P1**, **V1** and **V2**) had strikingly different reactivity against endogenous human PDI (the 57-kDa fluorescent band labeled with * in lane 1). **V1** and **V2**, two previously reported, highly potent irreversible inhibitors of parasitic/human cysteine proteases,[20] showed no apparent reactivity against human PDI even at 20 μM probe concentrations, whereas **P1** (an intended PTP inhibitor; Figure 1C; *vide infra*) showed potent and almost exclusive reactivity against human PDI at 5 μM concentration. A side-by-side comparison between **P1** and 16F16A, which is an alkyne-containing analog of 16F16 and had identical inhibitory activities against PDI,[5] showed that **P1** was at least as potent as, but more specific than, 16F16A in labeling endogenous PDI under our assay conditions. Interestingly, β-lactone probes such as **TR** and **TL**,[21] as well as the azanitrile-containing probe **AZ**,[23] previously shown to strongly label endogenous human fatty acid synthase (FAS) and cathepsin L (a cysteine protease) in mammalian cells, respectively, failed to label human PDI either. We therefore concluded **P1** might constitute a novel, cell-permeable small molecule inhibitor that could covalently modify endogenous PDI potently and selectively in human cancer cells. In order to unequivocally establish the 57-kDa band labeled by **P1** as endogenous human PDI, we carried out pull-down (PD) experiments on the **P1**-labeled MCF-7 proteome followed by Western blotting (WB) and LC-MS/MS analysis (Figure 2B and C); both results confirmed the 57-kDa band as human PDI. Two additional bands were also significantly enriched from the PD experiment, and they were subsequently identified as PDIA6 (48 kDa) and PDIA4 (73 kDa). Both proteins were previously known isoforms of human PDIs and possess similar active-site cysteine residues in their catalytic domains.[2] While PDIA4 is known to be localized to ER, the plasma membrane, and mitochondria, PDIA6 is localized predominantly to the nucleus of mammalian cells.[36] Further quantitative PD experiments showed that, although the endogenous expression levels of PDIA4 and PDIA6 were similar to that of PDI in MCF-7 cells, these two proteins were not labeled as efficiently by **P1** (SI Figure S9). We next used purified bovine PDI, which shares >95% sequence homology with human PDI, to establish the sensitivity of **P1** in labeling PDI *in vitro* (Figure 2D); as little as 50−100 nM of **P1** was sufficient to generate a strong fluorescent band. We further confirmed this labeling reaction was dependent upon PDI enzymatic activity, as small-molecule additives such as H_2O_2, DTT, and cystamine, all of which were previously known to modulate PDI enzymatic activity,[5,37,38] appeared to up/down-regulate the labeling intensity (SI Figure S2). We also directly labeled endogenous human PDI *in situ* in concentration- and time-dependent manners (Figure 2E); as low as 1−5 μM of **P1** was able to specifically label human PDI in as short as 15 min, indicating the PDI/**P1** reaction was rapid under physiological environments. Finally, in a competitive labeling experiment (Figure 2F), it was shown that the addition of excessive 16F16 to MCF-7 cells prior to **P1** was able to completely abolish PDI labeling, indicating that both 16F16 and **P1** likely targeted the same active-site cysteine residue(s) in human PDI.

Structure−Activity Relationship of P1 Analogs. Our newly discovered PDI-targeting compound **P1** was originally designed as a potential inhibitor of PTP1B (a human PTP linked to diabetes and obesity; see Figure 3A);[39] its phenyl vinyl sulfonate moiety was expected to serve as a phosphotyrosine mimic that might irreversibly label the nucleophilic cysteine residue in PTP1B active site.[19] Therefore, its exquisite *in situ* labeling profiles against human PDIs (PDI, PDIA4, and PDIA6) in MCF-7 cells were unexpected. To ensure that **P1** did not label endogenous PTP1B, we carried out labeling experiments both *in situ* using MCF-7 cells and *in vitro* using bovine PDI/recombinant PTP1B (Figure 3B and C); upon pull-down enrichment of the *in situ* **P1**-labeled MCF-7 proteome, we were unable to detect any **P1**-labeled

dx.doi.org/10.1021/cb4002602 | ACS Chem. Biol. XXXX, XXX, XXX−XXX

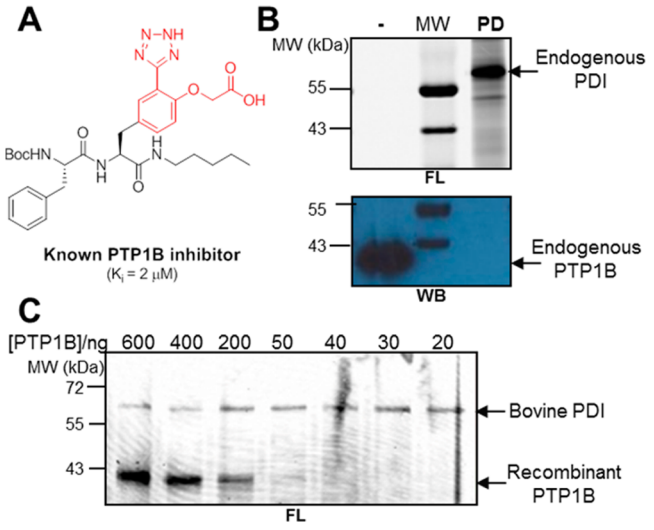

Figure 3. (A) Structure of a known PTP1B inhibitor from which **P1** was originally designed.[39] The group shown in red is a non-hydrolyzable bioisostere of phosphotyrosine. (B) In-gel fluorescence scanning (top) and Western blotting (bottom) of *in situ* **P1** (10 μM)-labeled MCF-7 cells, showing that endogenous PTP1B was not a target of **P1**. "−": negative control with cells treated with DMSO in place of **P1**. PD = pull-down sample of **P1**-treated MCF-7 proteome. In the WB (bottom), no PD was done on the negative control. The band labeled with an arrow indicates the endogenous PTP1B. (C) *In vitro* **P1** (100 nM) labeling of purified PTP1B in the presence of a fixed amount of bovine PDI (20 ng).

endogenous PTP1B by Western blotting using anti-PTP1B antibody (lane 3 in bottom gel of Figure 3B). This was despite the fact that PTP1B was highly expressed in MCF-7 cells (lane 1). In the *in vitro* experiments with purified proteins (Figure 3C), **P1** started to label PTP1B only when this protein was present in a much larger excess (>10×) than bovine PDI. On the basis of these experiments, we concluded that **P1** indeed did not label endogenous PTP1B in live MCF-7 cells.

In an effort to explore the structure−activity relationship (SAR) of **P1** in labeling/inhibiting endogenous human PDI, we next made two small libraries of **P1** analogs (Figure 4 and Table 1). We first made systematic modifications of the three key structural components, R_1, R_2, and R_3, in **P1** (Figure 4A). Docking results of **P1** binding to one of the catalytic domains in human PDI (a′) indicated that the phenyl ring in the R_1 group of **P1** engaged in $\pi-\pi$ interaction with PDI's Trp^{396} (insets in Figure 4A). In addition, the vinyl sulfonate in **P1** was projected into a cavity near Cys^{397} of PDI, therefore positioning itself in close proximity to initiate a covalent reaction. To further support possible modification of **P1** at $Cys^{397/400}$, we carried out LC-MS/MS protein sequencing experiments (SI Figure S10); the results showed >84% sequence coverage with the *in situ* **P1**-labeled human PDI (post-PD), and the only missing peptide being the one containing $Cys^{397/400}$. This indicates either one of these two residues was modified by **P1** as predicted by our docking results. Docking results indicated, however, that Cys^{397} was closer in distance to **P1** than Cys^{400}. Finally, cysteine-to-alanine mutants of human PDI transiently overexpressed in HEK293 cells were labeled by **P1** (SI Figure S10); the results unambiguously confirmed that Cys^{397} was indeed the site for **P1** modification. Subsequently, we replaced the phenyl vinyl sulfonate moiety in **P1** (e.g., R_{1a}) with coumarin vinyl sulfonate (R_{1b}), 2-fluoromethyl phenyl phosphate (FMPP, R_{1c}) and its coumarin analog (R_{1d}), and reduced vinyl sulfonate (R_{1e}). These variables were expected to delineate the effect of the electrophilic moiety in R_{1a} toward the labeling reaction. The Boc-(*S*)-Phe in **P1** (e.g., R_{2a}), another important structural component of the probe for PDI recognition, was replaced with four other aromatic acid building blocks (e.g., R_{2b} to R_{2e}). Lastly, the terminal alkyne-containing, five-carbon "click" tag in **P1**, R_{3a}, was replaced with either a smaller terminal alkyne linker (R_{3b}) or biotin (R_{3c}). In total, 10 additional compounds (**P2**−**P11**) were synthesized in this first library using schemes similar to what was shown in Figure 4A. We first compared the *in situ* proteome reactivity profiles of these newly synthesized probes in MCF-7 cells (Figure 4B). It became apparent that the phenyl vinyl sulfonate in **P1** was one of the most important determinants for PDI labeling, as **P3**/**P4**/**P5** did not show any noticeable fluorescent band at ∼57 kDa (lanes 3−5). **P5** was structurally identical to **P1**, except with a reduced vinyl sulfonate, which was incapable of being covalently modified by cysteine residues in the PDI active sites. Both **P3** and **P4** contain a 2-fluoromethyl aromatic phosphate, which would generate a highly reactive, electrophilic quinone methide intermediate only upon endogenous PTP hydrolysis.[40,41] It was previously shown that similarly designed, amino acid-containing probes were able to label many endogenous cellular proteins, including human PDI, but with little specificity in Hepatoma cells infected with Hepatitis C Virus (HCV).[42] The complete abolishment of PDI labeling by both **P3** and **P4** under our labeling conditions indicates that the presence of an electrophilic group in these probes alone was insufficient to achieve potent and specific *in situ* PDI targeting. Interestingly, **P2**, a coumarin analog of **P1**, showed a similar, but overall weaker, *in situ* labeling profile as **P1**, indicating the phenyl group in R_{1a} was optimized for PDI binding. Probes **P6** to **P10**, all of which showed a strongly fluorescent 57-kDa PDI band, produced similar *in situ* labeling profiles as **P1**, albeit with varying degrees of potency (judged by the fluorescent intensity of the 57-kDa band) and selectivity (judged by the presence of other fluorescent bands). This indicates both R_2 and R_3 groups in **P1** were nonessential elements, but provided additional recognition for specific *in situ* PDI binding/labeling (*vide infra*). We therefore concluded that a potent and selective PDI-targeting probe should possess both PDI-binding and suitable electrophilic moieties within the same molecular skeleton. We next tested all probes, including **P1**-**P11**, 16F16, 16F16A, and 16F16DC (an 16F16 analog that does not contain the electrophilic chloroacetyl group; see SI Figure S1), for their inhibitory property against bovine PDI using an insulin aggregation assay (inserted table in Figure 4A, and Figure 4C);[5,16] **P1** again emerged as one of the most potent inhibitors, with an apparent IC_{50} value of 1.7 ± 0.4 μM. Interestingly, in a side-by-side comparison, 16F16 was at least 40 times weaker in PDI inhibition (e.g., IC_{50} = 74 ± 6 μM) than **P1** under identical assay conditions (see Figure 4C). The other two 16F16 analogs, 16F16A and 16F16DC, also showed weak (IC_{50} = 108 ± 7 μM) or no inhibition against bovine PDI, respectively. Not surprisingly, **P3**/**P4**/**P5** showed minimal PDI inhibition even at 100 μM concentration, whereas **P2** and **P6**−**P11** showed IC_{50} values ranging from 1.1 to 5.3 μM. For example, **P11**, the biotin analog of **P1**, showed a slightly better *in vitro* inhibition than **P1** (IC_{50} = 1.1 ± 0.8 μM). This might be explained by its strong "avidity", due to the biotin in its structure, in nonspecific binding to bovine PDI *in vitro*. Whether or not the same phenomenon can be observed in live mammalian cells will need

dx.doi.org/10.1021/cb4002602 | *ACS Chem. Biol.* XXXX, XXX, XXX−XXX

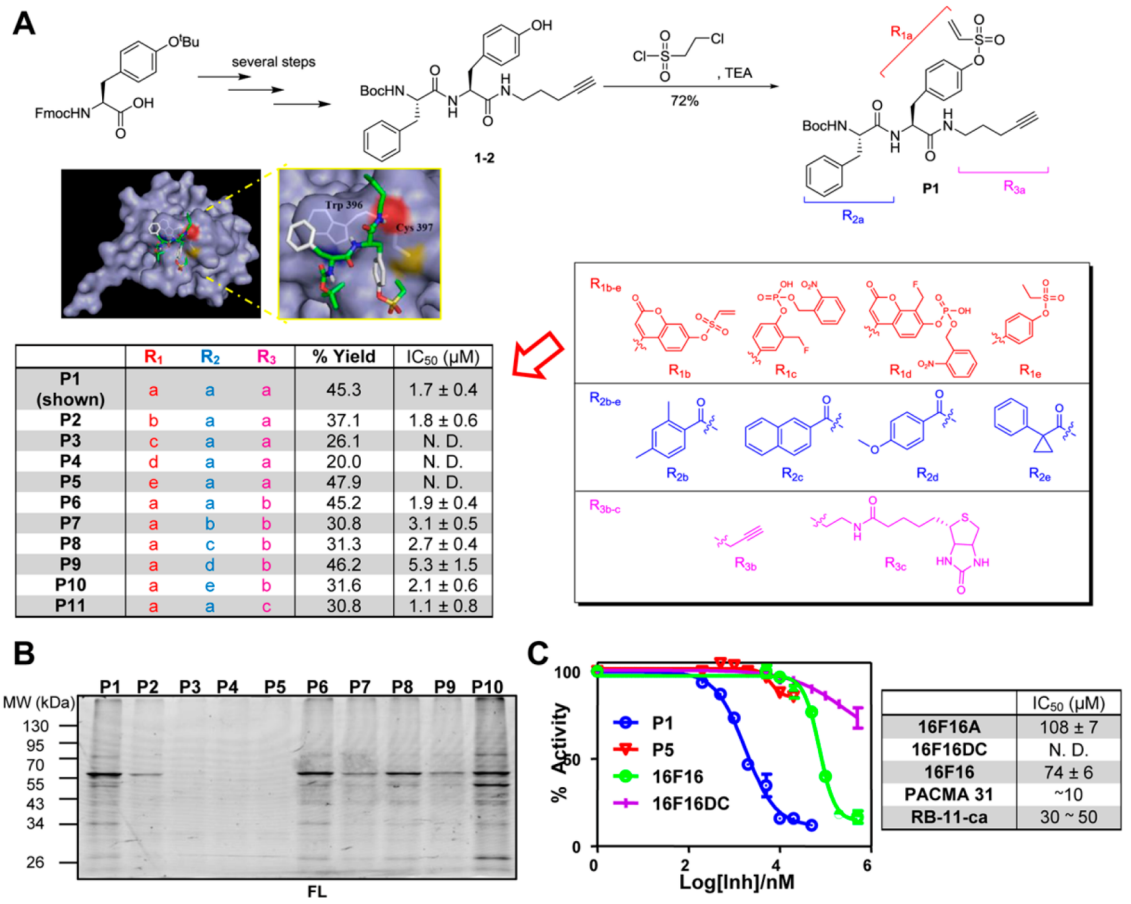

	R_1	R_2	R_3	% Yield	IC_{50} (μM)
P1 (shown)	a	a	a	45.3	1.7 ± 0.4
P2	b	a	a	37.1	1.8 ± 0.6
P3	c	a	a	26.1	N. D.
P4	d	a	a	20.0	N. D.
P5	e	a	a	47.9	N. D.
P6	a	a	b	45.2	1.9 ± 0.4
P7	a	b	b	30.8	3.1 ± 0.5
P8	a	c	b	31.3	2.7 ± 0.4
P9	a	d	b	46.2	5.3 ± 1.5
P10	a	e	b	31.6	2.1 ± 0.6
P11	a	a	c	30.8	1.1 ± 0.8

	IC_{50} (μM)
16F16A	108 ± 7
16F16DC	N. D.
16F16	74 ± 6
PACMA 31	~10
RB-11-ca	30 ~ 50

Figure 4. (A) Representative scheme showing the synthesis and structure of **P1** and its analogs (**P2** to **P11**; summarized in the inserted table), which contain three points of diversity (R_1, R_2, and R_3). The full structure of **P1** is shown. For complete structures of other analogs, see SI Table S1. Insets: docked structure of **P1** binding to the a′-domain of human PDI (left), and a close-up view (right) showing the proximity of the phenyl vinyl sulfonate group of **P1** and Cys^{397} in human PDI. The structure of PDI was taken from the Protein Data Bank (3UEM). (B) *In situ* proteome reactivity profiles of **P1** to **P10** (5 μM each) against MCF-7 cells. For **P3** and **P4**, upon addition of the probes, cells were first UV-irradiated (2 min) to uncage the photolabile group. For **P11** profiles, see SI Figure S5. (C) Insulin aggregation assay showing IC_{50} inhibition curves of representative compounds (**P1**, **P5**, 16F16, and 16F16DC; left) and the corresponding values (right). IC_{50} values of PACMA 31 and RB-11-ca. were extracted from reported literatures.[16,17] For IC_{50} value of other compounds, see the inserted table in part A. For other IC_{50} curves, see SI Figure S6.

to be further investigated. We therefore concluded that, at least under *in vitro* settings, **P1** was clearly more potent than 16F16, and, to our knowledge, one of the more potent small molecule inhibitors reported to date, against recombinant PDI.

In order to further delineate the SAR of **P1** in its inhibition against PDI, a secondary small molecule library was synthesized (Table 1), containing 14 compounds (**P12** to **P25**) with structural variations at the R_2 position. These compounds were again tested for their inhibition against bovine PDI using the insulin aggregation assay; the results indicate the IC_{50} values of all compounds were similar to **P1** (e.g., raging between 1.0 to 5.7 μM), which further confirms that even dramatic changes such as replacement of the chiral amino acid at the R_2 position in **P1** had marginal effects on the compound's overall inhibition against PDI *in vitro*.

Antiproliferation Activity of P1 in Different Cancer Cell Lines. Having successfully confirmed that **P1** as an *in vitro* PDI inhibitor was more potent than 16F16 under identical insulin aggregation assay conditions (e.g., > 40 times), and approximately 10 and 30 times more potent than PACMA 31 and RB-11-ca, respectively, based on previously reported values,[16,17] we next determined its cellular activities by measuring the GI_{50} (e.g., inhibition of 50% cell growth) values of **P1** against six different cancer cell lines. Weerapana et al. recently reported an GI_{50} value of 23.9 μM for RB-11-ca. against HeLa cells in an MTT antiproliferation assay.[17] The GI_{50} values for PACMA 31 was reported to be between 0.3 and 1.4 μM in various cancer cell lines. The exact GI_{50} value for 16F16, however, was not available, based on published data.[5,16] Again, in order to confirm PDI targeting by the probes (**P1** and 16F16A), and ensure accurate comparison of the tumor cell-killing activities of **P1** versus 16F16, both the *in situ* proteome profiles and the XTT antiproliferation activity of the probes were simultaneously determined (Figure 5A and B); *in situ* proteome reactivity profiles of **P1** in all six cell lines showed predominantly PDI labeling with some varying degrees of fluorescence, likely indicating the differences in the endogenous expression level of PDI in these cell lines. 16F16A, on the other hand, continued to show strong labeling of several other cellular proteins in addition to PDI, in all cell lines tested. Interestingly, **P1** and 16F16 showed comparable, low-micromolar inhibition of cell proliferation against all six cancer cells (Figure 5B), with apparent GI_{50} values of ~4 μM for both compounds. This finding is in contrast with our earlier *in vitro* results from the insulin aggregation assay, in which 16F16 showed comparatively weaker PDI inhibition. Our earlier *in situ*

dx.doi.org/10.1021/cb4002602 | ACS Chem. Biol. XXXX, XXX, XXX–XXX

Table 1. Structures of R_2-focused Library (P12-P25) and the Corresponding IC_{50} Values

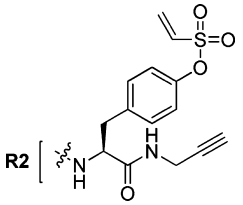

	R2	IC_{50} (μM)		R2	IC_{50} (μM)
P12		3.2 ± 0.5	P13		2.5 ± 0.5
P14		1.0 ± 0.4	P15		1.1 ± 0.3
P16		2.3 ± 0.6	P17	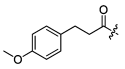	3.3 ± 2.0
P18		2.8 ± 1.0	P19		2.5 ± 2.2
P20		5.7 ± 1.4	P21		2.5 ± 0.5
P22		1.4 ± 0.3	P23		1.8 ± 0.4
P24		2.2 ± 0.4	P25		3.4 ± 0.6

proteome profiling results (Figure 5A) pointed to one possible explanation, that is, the improvement from *in vitro*-PDI inhibition to cell-proliferation inhibition by 16F16 might be due to its cellular targeting of other yet-to-be-identified cellular proteins. It is also possible that 16F16 inhibited endogenous PDI more effectively under native cellular environments.

To further delineate specific cellular targeting of PDI by **P1**/16F16, we used confocal fluorescence microscopy to visualize the colocalization of **P1**/16F16A with endogenous PDI in live MCF-7 cells (Figure 5C); upon treatment with the probe (1 μM), the labeled cells were fixed, followed by click chemistry with Rh-PEG-N_3, then imaged (pseudocolored in red; **P1**, panels 2 and 6; 16F16A, panels 10 and 14). The same cells were subsequently treated with anti-PDI antibodies following standard immunofluorescence (IF) protocols and imaged again (pseudocolored in green; panels 3 and 11). Merged images indicated that most of the fluorescence signals arisen from the **P1**/16F16A labeling indeed colocalized well with those from ER-localized human PDI (panels 4 and 12), as one might have expected. In addition, weaker but clear fluorescence signals from **P1**/16F16A were also detected within the cell nuclei. For **P1**, these imaging results appeared to be consistent with our earlier findings that **P1** labeled not only endogenous human PDI but also PDIA4 and the nucleus-localized PDIA6 (Figure 2B). For 16F16, on the other hand, our earlier *in situ* proteome profiling results had already confirmed the presence of other unknown cellular targets. The question of whether or not these unknown targets include other human PDIs such as PDIA6, however, remains to be further investigated. Notwithstanding, the potency and specificity of **P1** against human PDI both *in vitro* and in living cells indicate this probe might be further developed into a suitable small molecule-based, PDI-imaging agent.[43−45]

Conclusion. We have discovered a phenyl vinyl sulfonate-containing small molecule probe, **P1**, which showed relatively potent and selective covalent labeling of endogenous human

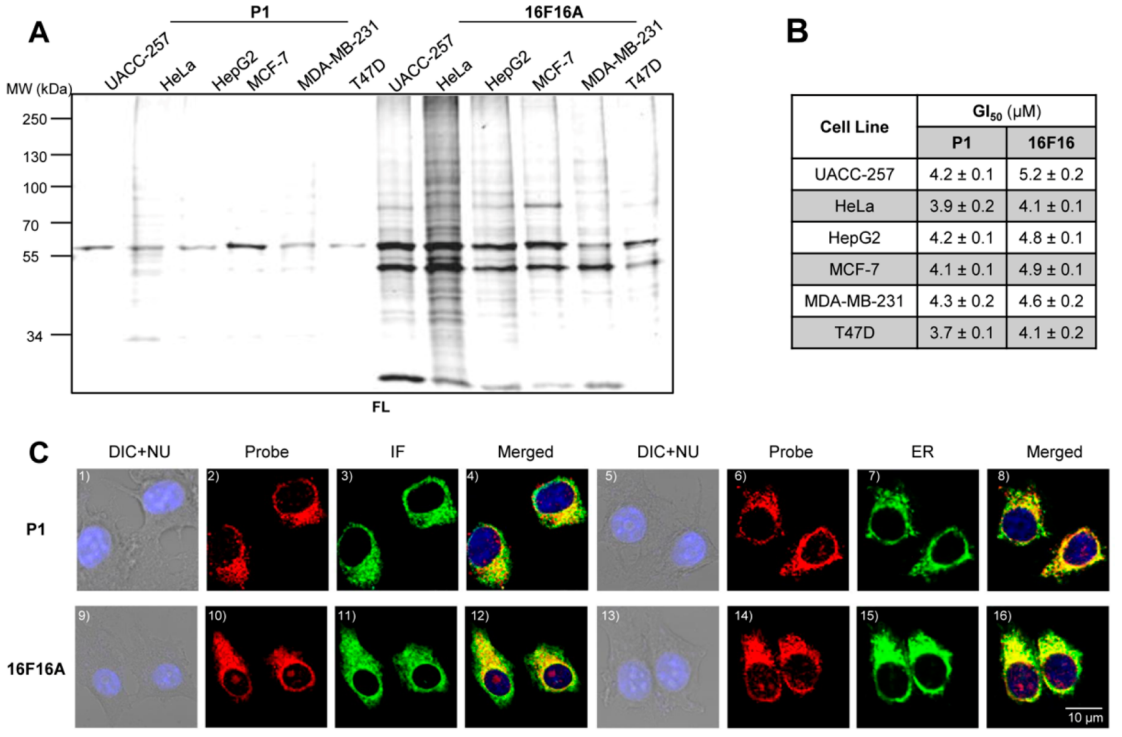

Cell Line	GI_{50} (μM)	
	P1	16F16
UACC-257	4.2 ± 0.1	5.2 ± 0.2
HeLa	3.9 ± 0.2	4.1 ± 0.1
HepG2	4.2 ± 0.1	4.8 ± 0.1
MCF-7	4.1 ± 0.1	4.9 ± 0.1
MDA-MB-231	4.3 ± 0.2	4.6 ± 0.2
T47D	3.7 ± 0.1	4.1 ± 0.2

Figure 5. (A) *In situ* proteome profiling of **P1** and 16F16A (5 μM) against six different cancer cell lines. (B) GI_{50} values of **P1** and 16F16 against six cancer cell lines. See SI Figure S7 for original GI_{50} plots. (C) Confocal microscopy showing the cellular localization of **P1** (panels 1−8) and 16F16A (panels 9−16).

dx.doi.org/10.1021/cb4002602 | *ACS Chem. Biol.* XXXX, XXX, XXX−XXX

PDI in live mammalian cells. Preliminary findings indicate **P1** was a fairly effective inhibitor when compared to some of the recently discovered PDI inhibitors.[5,14] We further showed **P1** may be a useful imaging agent to visualize endogenous human PDI in mammalian cells. During the course of our study, we did side-by-side detailed comparison of **P1** and 16F16, a compound previously shown to suppress apoptosis in a model of Huntington's disease, presumably through the inhibition of PDI.[5] We found that, while both **P1** and 16F16 possessed comparable antiproliferation activities in numerous cancer lines, **P1** was more potent than 16F16 in inhibiting *in vitro* PDI activities. This, together with the finding that **P1** labeled endogenous human PDI more specifically than 16F16A (an 16F16 analog) in live mammalian cells, points to the possibility that the cell-based biological activities displayed by 16F16, in contrast to previous report,[5] might have originated in part from other unknown cellular targets. Further studies, however, are needed to substantiate our speculation. The use of electrophilic chemical scaffolds demonstrated in the current study may provide a general concept to target other human PDIs in future.

METHODS

Synthesis. The synthesis of all compounds used in this study is reported in the Supporting Information.

General Procedures of *In Situ* Proteome Profiling, Target Validation by PD, WB, and LC-MS/MS. These protocols are modified based on previously reported procedures[21,44] and are provided in the Supporting Information.

Bovine PDI Experiments. For labeling of PDI with the probes, bovine PDI (25 ng) was incubated with different concentrations of a probe for 2 h. After incubation, click cocktail reagents were added (with Rh−N_3). The mixtures were gently shaken for 2 h. SDS-loading buffer was then added, and the solution was heated for 10 min at 95 °C. The proteins were resolved in a 10% SDS-PAGE gel, and the labeled bands were visualized by in-gel fluorescence scanning. To determine the effect of additives, PDI (100 ng) was treated with three different concentrations of DTT, H_2O_2, and cystamine for 1 h first in PBS buffer, respectively. **P1** (1 μM final concentration) was then added. All subsequent steps were the same as above-described. For PTP1B-competitive labeling experiments, different amounts of recombinant PTP1B were mixed with 20 ng PDI in Tris buffer. After 30 min, 100 nM **P1** was added, followed by click reaction. All subsequent steps were the same as above-described.

For PDI inhibition, the assay was carried out in 384-well plates according to literature procedures.[46] Each well contained 100 mM sodium phosphate and 0.2 mM EDTA, pH 7.0. PDI (10 ng) was first incubated with different concentration of probes (4% DMSO) in 20 μL buffer for 30 min at 37 °C. Then, insulin (0.16 mM final concentration) and dithiothreitol (1 mM final concentration) were added. The enzyme reaction was monitored at 650 nm on a Bioteck microplate reader. Experiments with 16F16 were done similarly side-by-side.

XTT Cell Proliferation Assay. Mammalian cell lines were seeded in 96-well plates at a concentration of 4000 cells per well. The cells were grown for 24 h before treatment with **P1** (or 16F16). After removing the growth medium by suction, different concentrations of **P1** in growth medium (100 μL, 1% DMSO) were added and the cells were incubated for 3 d at 37 °C/5% CO_2. Experiments with 16F16 were done similarly side-by-side. Subsequently, 50 μL of XTT reagent (1 mg mL^{-1}; Invitrogen) and PMS (0.025 mM; Sigma) were added, and the mixture was incubated at 37 °C/5% CO_2 for 6 h. The absorbance was measured at 450 nm, and background absorbance was measured at 650 nm using a Bioteck plate reader. Cells incubated with 1% DMSO served as positive control. Experiments were conducted in duplicate.

Live-Cell Imaging Experiments. MCF-7 cells were seeded in glass bottom dishes and grown to ∼60% confluence. The cells were incubated with 1 μM **P1** or 16F16A in fresh growth medium (400 μL). The cells were further incubated for 1 h at 37 °C/CO_2. Then, the cells were washed with PBS three times. Subsequently, cells were fixed with 3.7% formaldehyde in PBS for 20 min at 37 °C/CO_2, washed twice again, and permeabilized with 0.1% Triton X-100 in PBS for 15 min, then washed twice again. Subsequently, cells were treated with a freshly premixed click chemistry solution (150 μL; 2 μM Rh-PEG-N_3, 4 μM TBTA, 40 μM TCEP, 40 μM $CuSO_4$) for 2 h at RT with gentle shaking. Cells were washed with 2× PBS, several times PBS containing 0.1% Tween-20 and 0.5 mM EDTA, and 2× PBS. Cells were then blocked with 2% BSA, 0.05% Tween-20 in PBS for 1 h. For ER-localization experiments, cells were further incubated with ER tracker Green (Invitrogen, 0.3 μM final concentration) for 1 h and washed with PBS twice. For immunofluorescence experiments, cells were further incubated with PDI primary antibody (1:200 in 2% BSA, Santa Cruz, sc-166474) for 1 h at RT, washed once with 2% BSA, washed twice with PBS, and then incubated with FITC-conjugated antimouse IgG secondary antibody (1:100 in 2% BSA, Santa Cruz, sc-2010), then washed once with 2% BSA and twice with PBS. For both experiments the cells were incubated with nucleus stain (Hoechst, 0.2 μg mL^{-1} in final concentration) for 20 min and washed twice with PBS. Finally, the cells were washed and imaged.

ASSOCIATED CONTENT

Supporting Information

Other relevant experimental sections, characterizations of new compounds, and supplementary biological results. This material is available free of charge via the Internet at http://pubs.acs.org.

AUTHOR INFORMATION

Corresponding Author

*E-mail: chmyaosq@nus.edu.sg.

Notes

The authors declare no competing financial interest.

ACKNOWLEDGMENTS

Financial support was provided by National Medical Research Council (NMRC/1260/2010) and the Ministry of Education (MOE2012-T2-1-116) of Singapore. We also acknowledge the financial support from the Singapore−Peking−Oxford Research Enterprise (COY-15-EWI-RCFSA/N197-1). We thank E. Weerapana (Boston College, U.S.A.) for the generous gifts of the mammalian expression constructs of human PDI and mutants.

REFERENCES

(1) Ellgaard, L., and Ruddock, L. W. (2005) The human protein disulphide isomerase family: Substrate interactions and functional properties. *EMBO Rep. 6*, 28−32.

(2) Benham, A. M. (2012) The protein disulfide isomerase family: Key players in health and disease. *Antioxid. Redox Signal. 16*, 781−789.

(3) Nguyen, V. D., Wallis, K., Howard, M. J., Haapalainen1, A. M., Salo, K. E. H., Saaranen1, M. J., Sidhu, A., Wierenga1, R. K., Freedman, R. B., Ruddock, L. W., and Williamson, R. A. (2008) Alternative conformations of the x region of human protein disulphide-isomerase modulate exposure of the substrate binding b′ domain. *J. Mol. Biol. 383*, 1144−1155.

(4) Karala, A.-R., Lappi, A.-K., and Ruddock, L. W. (2010) Modulation of an active-site cysteine pK_a allows PDI to Act as a catalyst of both disulfide bond formation and isomerization. *J. Mol. Biol. 396*, 883−892.

(5) Hoffstrom, B. G., Kaplan, A., Letso, R., Schmid, R. S., Turmel, G. J., Lo, D. C., and Stockwell, B. R. (2010) Inhibitors of protein disulfide isomerase suppress apoptosis induced by misfolded proteins. *Nat. Chem. Biol. 6*, 900−906.

(6) Lee, S. O., Cho, K., Cho, S., Kim, I., Oh, C., and Ahn, K. (2010) Protein disulphide isomerase is required for signal peptide peptidase-mediated protein degradation. *EMBO J. 29*, 363−375.
(7) Dong, G., Wearsch, P. A., Peaper, D. R., Cresswell, P., and Reinisch, K. M. (2009) Insights into MHC class I peptide loading from the structure of the tapasin-ERp57 thiol oxidoreductase heterodimer. *Immunity 30*, 21−32.
(8) Gallina, A., Hanley, T. M., Mandel, R., Trahey, M., Broder, C. C., Viglianti, G. A., and Ryser, H. J. (2002) Inhibitors of protein disulfide isomerase prevent cleavage of disulfide bonds in receptor-bound glycoprotein 120 and prevent HIV-1 entry. *J. Biol. Chem. 277*, 50579−50588.
(9) Haefliger, S., Klebig, C., Schaubitzer, K., Schardt, J., Timchenko, N., Mueller, B. U., and Pabst, T. (2011) Protein disulfide isomerase blocks CEBPA translation and is up-regulated during the unfolded protein response in AML. *Blood 117*, 5931−5940.
(10) Goplen, D., Wang, J., Enger, P. O., Tysnes, B. B., Terzis, A. J. A., Laerum, O. D., and Bjerkvig, R. (2006) Protein disulfide isomerase expression is related to the invasive properties of malignant glioma. *Cancer Res. 66*, 9895−9902.
(11) Roth, R. A. (1981) Bacitracin—An inhibitor of the insulin degrading activity of glutathione-insulin transhydrogenase. *Biochem. Biophys. Res. Commun. 98*, 431−438.
(12) Ryser, H. J., Levy, E. M., Mandel, R., and DiSciullo, G. J. (1994) Inhibition of human immunodefficiency virus infection by agents that interfere with thiol-disulfide interchange upon virus−receptor interaction. *Proc. Natl. Acad. Sci. U.S.A. 91*, 4559−4563.
(13) Dickerhof, N., Kleffmann, T., Jack, R., and McCormick, S. (2011) Bacitracin inhibits the reductive activity of protein disulfide isomerase by disulfide bond formation with free cysteines in the substrate-binding domain. *FEBS J. 278*, 2034−2043.
(14) Karala, A. R., and Ruddock, L. W. (2010) Bacitracin is not a specific inhibitor of protein disulfide isomerase. *FEBS J. 277*, 2454−2462.
(15) Khan, M. M., Simizu, G. S., Lai, N. S., Kawatani, M., Shimizu, T., and Osada, H. (2011) Discovery of a small molecule PDI inhibitor that inhibits reduction of HIV-1 envelope glycoprotein gp120. *ACS Chem. Biol. 6*, 245−251.
(16) Xu, S., Butkevich, A. N., Yamada, R., Zhou, Y., Debnath, B., Duncan, R., Zandi, E., Petasis, N. A., and Neamati, N. (2012) Discovery of an orally active small-molecule irreversible inhibitor of protein disulfide isomerase for ovarian cancer treatment. *Proc. Natl. Acad. Sci. U.S.A. 109*, 16348−16353.
(17) Banerjee, R., Pace, N. J., Brown, D. R., and Weerapana, E. (2013) 1,3,5-Triazine as a modular scaffold for covalent inhibitors with streamlined target identification. *J. Am. Chem. Soc. 135*, 2497−2500.
(18) Raturi, A., Vacratsis, P. O., Seslija, D., Lee, L., and Mutus, B. (2005) A direct, continuous, sensitive assay for protein disulphide isomerase based on fluorescence self-quenching. *Biochem. J. 391*, 351−357.
(19) Liu, S., Zhou, B., Yang, H. H., He, Y., Jiang, Z. X., Kumar, S., Wu, L., and Zhang, Z. Y. (2008) Aryl vinyl sulfonates and sulfones as active site-directed and mechanism-based probes for protein tyrosine phosphatases. *J. Am. Chem. Soc. 130*, 8251−8260.
(20) Yang, P. -Y., Wang, M., He, C. Y., and Yao, S. Q. (2012) Proteomic profiling and potential cellular target identification of K11777, a clinical cysteine protease inhibitor, in *Trypanosoma brucei*. *Chem. Commun. 48*, 835−837.
(21) Yang, P. -Y., Liu, K., Ngai, M. H., Lear, M. J., Wenk, M. R., and Yao, S. Q. (2010) Activity-based proteome profiling of potential cellular targets of orlistat—An FDA-approved drug with anti-tumor activities. *J. Am. Chem. Soc. 132*, 656−666.
(22) Bottcher, T., and Sieber, S. A. (2008) β-Lactones as privileged structures for the active-site labeling of versatile bacterial. *Angew. Chem., Int. Ed. 47*, 4600−4603.
(23) Yang, P. -Y., Wang, M., Li, L., Wu, H., He, C. Y., and Yao, S. Q. (2012) Design, synthesis, and biological evaluation of potent azadipeptide nitrile inhibitors and activity-based probes as promising anti-*Trypanosoma brucei* agents. *Chem.—Eur. J. 18*, 6528−6541.
(24) Loser, R., Frizler, M., Schilling, K., and Gutschow, M. (2008) Azadipeptide nitriles: Highly potent and proteolytically stable inhibitors of papain-like cysteine proteases. *Angew. Chem., Int. Ed. 47*, 4331−4334.
(25) Wirth, T., Schmuck, K., Tietze, L. F., and Sieber, S. A. (2012) Duocarmycin analogues target aldehyde dehydrogenase 1 in lung cancer cells. *Angew. Chem., Int. Ed. 51*, 2874−2877.
(26) Kaschani, F., Clerc, J., Krahn, D., Bier, D., Hong, T. N., Ottmann, C., Niessen, S., Colby, T., van der Hoorn, R. A. L., and Kaiser, M. (2012) Identification of a selective, activity-based probe for glyceraldehyde 3-phosphate dehydrogenases. *Angew. Chem., Int. Ed. 51*, 5230−5233.
(27) Pace, N. J., Pimental, D. R., and Weerapana, E. (2012) An inhibitor of glutathione S-transferase omega 1 that selectively targets apoptotic cells. *Angew. Chem., Int. Ed. 51*, 8365−8368.
(28) Evans, M. J., and Cravatt, B. F. (2006) Mechanism-based profiling of enzyme families. *Chem. Rev. 106*, 3279−3301.
(29) Uttamchandani, M., Li, J., Sun, H., and Yao, S. Q. (2008) Activity-based profiling: New developments and directions in functional proteomics. *ChemBioChem 9*, 667−675.
(30) Fonovic, M., and Bogyo, M. (2008) Activity-based probes as a tool for functional proteomic analysis of proteases. *Exp. Rev. Proteomics 5*, 721−730.
(31) Heal, W. P., Dang, T. H. T., and Tate, E. W. (2011) Activity-based probes: Discovering new biology and new drug targets. *Chem. Soc. Rev. 40*, 246−257.
(32) Sletten, E. M., and Bertozzi, C. R. (2009) Bioorthogonal chemistry: Fishing for selectivity in a sea of functionality. *Angew. Chem., Int. Ed. 48*, 6974−6998.
(33) Kalesh, K. A., Shi, H., Ge, J., and Yao, S. Q. (2010) The use of click chemistry in the emerging field of catalomics. *Org. Biomol. Chem. 8*, 1749−1762.
(34) Kolb, H. C., and Sharpless, K. B. (2003) The growing impact of click chemistry on drug discovery. *Drug Discovery Today 8*, 1128−1137.
(35) Meldal, M., and Tornøe, C. W. (2008) Cu-catalyzed azide-alkyne cycloaddition. *Chem. Rev. 108*, 2952−3015.
(36) http://www.hprd.org (accessed March 15, 2013).
(37) Lundström, J., and Holmgren, A. (1990) Protein disulfide isomerase is a substrate for thioredoxin reductase and has thioredoxin-like activity. *J. Biol. Chem. 265*, 9114−9120.
(38) Darby, N. J., Freedman, R. B., and Creighton, T. E. (1994) Dissecting the mechanism of protein disulfide isomerase catalysis of disulfide bond formation in a model peptide. *Biochemistry 33*, 7937−7947.
(39) Liljebris, C., Larsen, S. D., Ogg, D., Palazuk, B. J., and Bleasdale, J. E. (2002) Investigation of potential bioisosteric replacements for the carboxyl groups of peptidomimetic inhibitors of protein tyrosine phosphatase 1B: Identification of a tetrazole-containing inhibitor with cellular activity. *J. Med. Chem. 45*, 1785−1798.
(40) Kalesh, K. A., Tan, L. P., Liu, K., Gao, L., Wang, J., and Yao, S. Q. (2010) Small molecule probes that target Abl kinase. *Chem. Commun. 46*, 589−591.
(41) Ge, J., Li, L., and Yao, S. Q. (2011) A self-immobilizing and fluorogenic unnatural amino acid that mimics phosphotyrosine. *Chem. Commun. 47*, 10939−10941.
(42) Blais, D. R., Brulotte, M., Qian, Y., Belanger, S., Yao, S. Q., and Pezacki, J. P. (2010) Activity-based proteome profiling of hepatoma cells during hepatitis C virus replication using protease substrate probes. *J. Proteome Res. 9*, 912−923.
(43) Yang, K. S., Budin, G., Reiner, T., Vinegoni, C., and Weissleder, R. (2012) Bioorthogonal imaging of aurora kinase A in live cells. *Angew. Chem., Int. Ed. 51*, 6598−6603.
(44) Shi, H., Zhang, C. -J., Chen, G. Y. J., and Yao, S. Q. (2012) Cell-based proteome profiling of potential dasatinib targets by use of affinity-based probes. *J. Am. Chem. Soc. 134*, 3001−3014.
(45) Li, L., Ge, J., Wu, H., Xu, Q. -H., and Yao, S. Q. (2012) Organelle-specific detection of phosphatase activities with two-photon

fluorogenic probes in cells and tissues. *J. Am. Chem. Soc. 134*, 12157−12167.

(46) Smith, A. M., Chan, J., Oksenberg, D., Urfer, R., Wexler, D. S., Ow, A., Gao, L., McAlorum, A., and Huang, S. -G. (2004) A high-throughput turbidometric assay for screening inhibitors of protein disulfide isomerase activity. *J. Biomol. Screen. 9*, 614−620.